A novel split cycle internal combustion engine with integral waste heat recovery

Guangyu Dong*, Robert Morgan and Morgan Heikal

School of Computing, Engineering and Mathematics, University of Brighton, BN2 4GJ, United Kingdom. G.Dong@brighton.ac.uk +441273641950

* Corresponding author.

Keywords

Split cycle
Isothermal compression
Isobaric combustion
Heat recuperation
Waste heat recovery

Abstract

To achieve a step improvement in engine efficiency, a novel split cycle engine concept is proposed. The engine has separate compression and combustion cylinders and waste heat is recovered between the two. Quasi-isothermal compression of the charge air is realized in the compression cylinder while isobaric combustion of the air/fuel mixture is achieved in the combustion cylinder. Exhaust heat recovery between the compression and combustion chamber enables highly efficient recovery of waste heat within the cycle. Based on cycle analysis and a one-dimensional engine model, the fundamentals and the performance of the split thermodynamic cycle is estimated. Compared to conventional engines, the compression work can be significantly reduced through the injection of a controlled quantity of water in the compression cylinder, lowering the gas temperature during compression. Thermal energy can then be effectively recovered from the engine exhaust in a recuperator between the cooled compressor cylinder discharge air and the exhaust gas. The resulting hot high pressure air is then injected into a combustor cylinder and mixed with fuel, where near isobaric combustion leads to a low combustion temperature and reduced heat transferred from the cylinder wall. Detailed cycle simulation indicates a 32% efficiency improvement can be expected compared to the conventional diesel engines.

1. Introduction

The internal combustion engine (ICE) has been the incumbent power source for road transport applications for over 100 years. The high power density, good transient response and low cost make the ICE an excellent fit with the needs of road vehicles in an environment with an abundant supply of low cost liquid fossil fuels [1-3]. However, climate change and diminishing stocks of petroleum have led to a drive for higher efficiency solutions [4, 5]. Alternative power converters such as fuel cells and batteries and increased electrification of the transmission between the prime mover and the wheels and downsizing of the ICE have also been proposed to improve the vehicle system performance [6]. Fuel cells and electrification are attractive for the passenger cars, but the high load factor of commercial vehicles is particularly challenging to such alternative powertrains [7, 8]. Recent research [9] has shown improvements to the thermal efficiency of the ICE offers the most effective means of reducing energy consumption when compared to other solutions on the basis of both cost and overall efficiency (including fuel processing and logistics chain efficiencies).

Incremental improvements in the ICE efficiency through friction reduction and improvements in the combustion system will continue but savings will become increasingly difficult and costly [10]. Waste heat recovery such as organic Rankine cycles [9] and open gas and steam cycles [11] have been proposed and could deliver improvements of the order of 2-5%. Alternative combustion systems, such as Low temperature combustion to reduce heat losses [12] could also improve efficiency. However, these approaches, even when combined with waste heat recovery are likely to yield a maximum system efficiency of 45-50% [13]. Further improvements to efficiencies beyond 50% require a fundamental change to the ICE cycle.

The splitting of the compression and expansion strokes into separate cylinders has the potential to greatly improve the overall cycle efficiencies through:

1) Reduction of the compression work by induction into a cool cylinder or direct cooling of the charge air during compression
2) Decoupling of the compression and expansion strokes effectively enabling a Miller cycle
3) High pressure waste heat recovery between the compression and combustion cylinders

The concept of splitting the ICE cycle into separate cylinders is not new, and was first described by Ricardo in 1908 [14]. Coney [15] evolved the cycle to add isothermal compression and high pressure

recuperation for stationary power applications. Water injection into the compression cylinder was proposed to achieve isothermal compression. A break efficiency of 60% was predicted using cycle simulation, but the contribution of the various features of the cycle was not described. Scuderi [16] proposed an alternative concept for road transport applications, that utilised a cool compressor cylinder and separate combustion cylinder with a close coupled transfer port. Both concepts were taken to lab demonstration, but were not commercialised. More recently, Atkins [17] has suggested a variant of the Coney engine that uses liquid nitrogen to cool the compressor, exploiting both the latent and sensible heat of the cryogenic fluid. It is claimed this overcomes the difficulties of carrying a water handling system on a road vehicle.

In this paper, we analyse the split cycle engine in detail to understand the contribution of various features of the cycle to the overall efficiency. Classical analysis is first used to investigate the global trade offs of compression ratio and waste heat recovery on a reciprocating split cycle engine. Full cycle analysis is then used to investigate in detail key features of the cycle and the impact on the engine architecture. The paper concludes with a discussion on the potential of a split cycle engine in road transport and stationary applications.

Nomenclature

a	droplet surface area (m^2/kg)	ER	expansion ratio	Q_{LH}	Fuel heat release amount (kJ)	V	volume
atdc	after top dead centre	EVC	exhaust valve close timing	Q_{RE}	recuperated heat (kJ)	**Greeks**	
AFR	air fuel ratio	EVO	exhaust valve open timing	S	entropy	ε	specific heat ratio
C	Isothermal index	h	*enthalpy (kJ/kg)*)	T	temperature (K)	σ	recuperator effectiveness
CA	crank angle	IVC	Intake valve close timing	T_{in}	Intake air temperature (K)	η	thermal efficiency
C_v	specific heat under constant volume	IVO	Intake valve open timing	T_{out}	Outlet air temperature (K)	**Subscripts**	
C_p	specific heat under constant pressure	k	isentropic exponent	Δ	difference	LH	fuel lower heating value
CR	compression ratio	p	pressure	u	heat transfer coefficient	RE	heat recuperation

2. Engine structure and theatrical thermodynamic cycle analysis

2.1 Description of the split engine cycle

A schematic of the 'isoengine' type of split cycle engine is shown in Fig. 1. Ambient air at stage point 1 is pre-compressed in the turbocharger, and then sent to the reciprocating compression cylinder (2). A certain amount of water is injected into the cylinder to cool down the air during compression, resulting in a quasi-isothermal compression process. After the compression stage (3), a high-pressure two-phase water/air mixture leaves the isothermal compressor, and the water is recovered in a separator. The liquid water is cooled and sent back to a water tank (5). A recuperator is installed downstream the separator to heat the high-pressure air (4). Within the recuperator, the air is heated by the exhaust flow (7), and then an intra-cylinder heat recovery process is achieved.

After the recuperation process (6), the fully preheated compressed air is fed to the combustion cylinders. As the combustion chamber intake valve opening time (IVO) is near to top dead centre (TDC), the diffusion of the combustion flame occurs in the expansion stroke of the cylinder. As a result, the combustion peak pressure is not increased significantly and a quasi-isobaric combustion process can be assumed. At the end of the expansion stage, the cylinder pressure is very close to the pressure in the exhaust pipe (7), so the exhaust stroke can be assumed as nearly isobaric as well. Based on the above processes, a complete split cycle is achieved.

2.2 Thermodynamic cycle analysis of the split cycle engine

The introduction of the split cycle engine indicates that both the combustion and exhaust stroke are nearly isobaric, and the expansion stroke can be treated as nearly adiabatic. The thermodynamic characteristics of the split cycle engine are therefore very similar to the Brayton cycle [18, 19]. A comparison between a simple Brayton cycle, recuperated Brayton cycle, ideal iso-thermal split cycle and quasi-isothermal split cycle is shown in Table 1.

For the Brayton cycle, the efficiency of the cycle is decided by the compression ratio (CR) only. The ideal efficiency of the cycle is greater than 60% when the CR is greater than 15. However, this efficiency can be improved, especially under a lower CR conditions by recovering waste heat through a recuperator to pre-heat the charge air post compression. The efficiency of this cycle is decided not only by the compression ratio, but also the regenerator effectiveness and the amount of heat released from the combustion process. In this thermodynamic cycle, the compressed air will be pre-heated by the exhaust gas. The recuperation process only works when the exhaust temperature T_4 is higher

than the compressed air temperature T_2. According to Table 1, the following relationship should be satisfied:

$$\underbrace{(T_1 \cdot CR^{k-1} + \frac{Q_{LH}}{C_p}) / CR^{k-1}}_{T_4} > \underbrace{T_1 \cdot CR^{k-1}}_{T_2} \quad (1)$$

Clearly, with the increase of T_2 and the decreases of T_4, the efficiency of this cycle cannot be improved when a higher CR is applied. To find the available compression ratio range, the variables x and l are defined as:

$$x = CR^{k-1}, l = \frac{Q_{LH}}{C_p T_1} \quad (2)$$

So the relationship 1 can be rearranged as:

$$\left(x - 1/2\right)^2 - (l - 1/4) < 0 \quad (3)$$

Assuming a 2,200 K maximum combustion temperature which represents the normal heat release case in diesel engines [20], and a recuperator effectiveness of 0.8, the available compression ratio range is shown in Fig. 2. Under such conditions, recuperation only can be achieved when the CR value is lower than 15.6, lower than the normal CR value is 17 or higher for a diesel engine.

The split thermodynamic cycle, enables a much wider recuperation range than can be achieved with a recuperated Brayton cycle. In an ideal Split cycle, an isothermal compression process is applied. Thus the compression air temperature T_2 is the same as the initial intake air temperature T_1. Then the temperature T4 can be expressed as:

$$T_4 = (T_1 + (Q_{LH} + Q_{RE}) / C_p) / CR^{(K-1)} \quad (4)$$

The expansion temperature T_4 is therefore always higher than T_2 regardless of the compression ratio. As a result, the recuperation process can be achieved throughout the compression ratio range.

For the real split cycle engine, the compression process is assumed to be quasi-isothermal. As a result, the T_4 is not always higher than the compression temperature T_2' and a limited recuperation range exists for this cycle.

The temperature $T_{2'}$ is strongly affected by the heat transfer process between the injected water and the intake air. The effect of heat transfer from the air to water droplets can be represented by a modified form of the well-known relationship for an ideal gas undergoing isentropic compression or expansion [21]. The modified equation is derived from the First Law of Thermodynamics in a similar way to the original equation, yielding:

$$\frac{T_{2'}}{T_1} = CR^{(K-1)\bullet \exp\left[-\frac{ua}{c_p}\left(1-\frac{T_w}{T_1}\right)\Delta t\right]} \quad (5)$$

Equation (5) relates the change of air temperature and pressure during a time interval Δt, with the exponential function representing the effect of heat transfer to the droplets. T_w is the mean spray water temperature, C_p is the specific heat of the air in the cylinder, K is the isentropic index, u is the heat transfer coefficient between the air and the water droplets and *a* is the droplet surface area per kg of air. If $u_a \bullet \Delta t$ is near zero then the exponential function tends to unity and the temperature ratio tends to the unmodified isentropic relationship. On the other hand if $u_a \bullet \Delta t$ is large then T_2 rapidly converges on T_w. Since the parameters of the exponential function depend on time and may undergo rapid changes during compression, the above expression should only be applied to small time intervals and small pressure ratios. Here, we define the isothermal index C as:

$$\mathrm{C} = \exp\left[-\frac{ua}{c_p}\left(1-\frac{T_w}{T_1}\right)\Delta t\right] \quad (6)$$

Then the value of C is directly affected by the water injection amount. When the water injection rate is high, the value of C is close to 0 and the compression process can be treated as nearly isothermal. On the contrary, the value is close to 1 and an isentropic compression process can be assumed. Accordingly, the temperature of T_2 and T_4 can be expressed as:

$$T_{2'} = T_1 \cdot CR^{(K-1)\bullet C} \quad (7)$$

$$T_4 = \frac{T_1 \cdot CR^{(K-1)C} + (Q_{RE} + Q_{LH})/C_p}{CR^{(K-1)}} \quad (8)$$

According to the above two equations, we can conclude that T_4 is not necessarily higher than T_2. However, comparing to the case of the recuperated Brayton cycle, the compression temperature $T_{2'}$ is

much lower. Given the same compression ratio, the recuperation available range in the split cycle engine is wider than the recuperated Brayton cycle.

Fig. 3 shows the efficiency comparison between the above 4 cycles. Here a recuperator effectiveness is defined as $\sigma = (T_{2'} - T_2) / (T_4 - T_2)$ to calculate the recuperated heat Q_{RE}. The σ is assumed to be 0.8 which represent the performance typical of a commercial recuperator. The variable C is assumed to be 0.45 which represents moderate cooling of the air by the injected water. From the Fig. 3 it can be seen that, compared to the simple Brayton cycle, the efficiency of the recuperated Brayton cycle can be improved when the compression ratio is less than 15.6. However a further improvement can be achieved on the split cycle engine until the compression ratio is 23.7. Within this range, the ideal split cycle efficiency can exceed 60%. This analysis demonstrates the split cycle engine is expected to significantly improve the efficiency when it is applied to conventional reciprocating engines. To analyse the engine performance in detail, a one dimensional model is constructed and discussed in the following sections.

3. Engine modelling and experimental validation

A numerical model of the system was realised using the LMS Imagine.Lab AMESim [22], a software for the simulation and analysis of one-dimensional systems. The IFP engine system module is in particular devoted to the development of internal combustion engine models, allowing the simulation of the considered engine system in both stationary and transient conditions [23]. Fig. 4 shows the layout of the proposed split cycle engine model. To simulate the effect of the water injection, the spray heat transfer model in the IFP engine package was applied, and validated by the experimental data achieved on a prototype engine [24].

Concerning the separator, there is no available model template available in the AMEsim environment. However, considering that the efficiencies of commercial water separators are very close to 100%, we assumed that the water was completely removed from the air-water mixtures without changing the status of the flow transfer from the compression chamber to the recuperator. Accordingly, the compression chamber is connected to a dummy combustion chamber in the model, and then the mixture flow status such as temperature and pressure can be collected in real time and used to define the status of the pure air flow sent to the real combustion chamber. Also, the flow rate of the pure air can be calculated by a water percentage sensor which is coded with C in the AMEset environment

[25]. To predict the recuperator behaviour, a heat exchanger model is applied. Then the heat transfer between the intake air and exhaust gas can be evaluated. Finally, the combustion behaviour is predicted by the combustion chamber which is based on the IFP engine package in AMEsim. The heat release process and the heat transfer behaviours in the combustion chamber are validated and calibrated by the experimental data collected on a conventional diesel single cylinder engine. The specifications of the split cycle engine modelled are shown in Table 2.

Fig. 5 shows a comparison between the split cycle engine and the conventional diesel engine. As shown in fig.5 (a), the pressure in the combustion chamber of the split cycle engine increased dramatically when the intake valve opened, but the rate of pressure rise at the start of combustion is much lower compared to a conventional diesel engine, leading to a quasi-isobaric combustion process. The fuel injection timing on the split cycle is retarded to avoid the start of combustion coinciding with an open intake valve [15], leading to backflow into the intake manifold. Subsequently the combustion phase is delayed to the expansion stroke as shown in Fig. 5 (b). Due to the retarded combustion, the peak heat transfer rate is much lower than in a conventional diesel engine, whereas the rate falls more slowly during the expansion stage due to late combustion, as can be seen in fig. 5 (c). The T-S diagrams of both engines can be seen in Fig. 5 (d). Due to the quasi-isothermal compression and recuperation process, the work, represented by the area bound by the TS diagram is higher for the same heat addition from combustion resulting in a 13% total efficiency improvement. Details of cycle will be discussed in the following sections.

4. Results and discussions

4.1. Evaluation of the isothermal compression process

Isothermal compression can yield significant savings in compression work compared to the adiabatic (isentropic) compression, where more work is needed to compress the hotter gas. The effect of the injection of water into the compressor chamber, for a 350K intake air temperature and 2 bar initial pressure is shown in Fig. 6. The adiabatic case results in a 92 bar final pressure at the position of EVO for a CR of 18. When a 20g/s water injection applied, the compression pressure is significantly decreased for the same compression ratio. When the CR value increased to 31.5, the same final pressure is achieved as the adiabatic case, to provide equivalent combustor inlet pressure. Since the compression stroke length is fixed, the compression work is decided by the in-cylinder pressure

during the compression. Compared to the pressure curve of adiabatic compression, the pressure is decreased when the water injection is applied. The water injection therefore reduces both the compression temperature and the consumed work on the split cycle engine.

Under different compression ratios (CR), the effect of the water injection rate on the work consumption is shown in Fig. 7 (a). When the water injection rate increases, the work saving also increases. Similarly, the consumed work is greatest under high compression ratio conditions. For an 80g/s water injection rate, 15.7% of the compression work can be saved with a CR value of 22. However, the percentage does not increase significantly when the injection rate is higher than 40g/s. The effect of the water injection rate on the in-cylinder temperature can be seen in Fig.7 (b), a significant decrease is observed even when the water injection is as low as 5g/s. With a CR value of 18, the compressed air temperature is as low as 380K for a 37g/s of water injection, only slightly higher than the 350K intake temperature. The water injection rate should therefore be calibrated carefully to achieve quasi-isothermal compression to avoid excessive water injection and associated parasitic losses.

4.2. Heat recovery system evaluation

In section 2.2, we assumed a constant recuperation effectiveness σ in the theoretical model. However, the effectiveness will vary depending on the operating conditions. The specifications of the recuperator can be seen in table 3. A one-dimensional recuperation system model was developed via AMEsim, and validated by the recuperator data modelled by Oliverira [26].

According to the definition of the recuperator effectiveness σ in section 2.2, the σ is mainly affected by the fresh air inlet temperature $T_{2'}$ (which is the inlet air temperature of the recuperator, slave side), and exhaust outlet temperature T_4. As discussed in section 2, $T_{2'}$ is the temperature at the end of quasi-isothermal compression process, and the T_4 is the temperature at the end of the expansion process (which is the inlet exhaust temperature of the recuperator master side). Given a fixed temperature $T_{2'}$, the compression ratio is the key factors which affect the effectiveness. Figs. 8 (a) and (b) show the one dimensional temperature distribution within the recuperator for compression ratios (CR) 20 and 25 respectively. From the inlet to the outlet of the recuperator, 10 nodes are applied with a fixed interval of 60mm (1/10 of the total length), and then the one dimension temperature distribution is calculated. The air-fuel ratio was fixed at 18 and a 10g/s water injection is applied. As

the water injection rate is the same, the air inlet temperatures $T_{2'}$ is nearly the same under these two cases. In Fig.8 (a), it can be seen that the temperature difference between T_4 and T_2, is 69K when the CR is 20. But this difference increases to 198K when the CR increases to 25 as seen in Fig. 8 (b). Due to the effect of the heat transferred form the combustion cylinder, the recuperator temperature is pinched at 0.6-0.7 normalised distance from the cold end. The above results indicate that the recuperator effectiveness decreases when the CR is increased.

To investigate this issue, the recuperator wall temperature was analysed. As seen in both cases (Fig. 8), the wall temperature is very close to the expansion temperature T_4. So it can be deduced that a higher expansion temperature leads to a higher wall transfer heat losses. Accordingly, the rate of temperature rise at the outlet side of the recuperator is lower when the expansion temperature is higher. As a result, it can be deduced that the recuperator effectiveness decreases under the higher compression ratio condition.

4.3 Combustion process

For the split thermodynamic cycle, the cycle efficiency is decided by 3 independent parameters; the isothermal index C, the recuperator effectiveness σ, and the combustion heat release Q_{LH}. For the real engine, the value C is mainly determined by the water injection rate, the recuperator effectiveness σ is determined by the recuperator specifications and its operation conditions. Q_{LH} directly affects the peak combustion temperature T_3. Setting the compression ratio at 16 and keeping the water injection rate at 25g/s, the effect of air-fuel ratio λ is discussed in this section.

Fig. 9 (a) shows the pressure curves with different air-fuel ratios. In contrast to the conventional engine, a moderate rate of pressure rise is observed on the split cycle engine. This phenomenon is mainly due to the intake valve open timing being close to the TDC, and the combustion occurring during the expansion process. The combustion process for the split cycle engine can be treated as near isobaric. Given a certain thermal load constraint, such a combustion process enables a higher compression ratio, and high cycle thermal efficiency. Fig. 9 (b) shows the peak temperatures for different λ values. When the air-fuel ratio is 16, the peak combustion temperature is still less than 1,600K, which is lower than conventional diesel engines. Referring to the diesel engine and split cycle engine model mentioned in section 3, a comparison between the two cycles is discussed below.

Given a fix air-fuel ratio of 17, and maintaining the compression ratios of 16, the in-cylinder energy balance is compared. Fig. 10 (a) and (b) are the energy balances within the combustion cylinders of the conventional and the split engine. In a split cycle engine, the cumulative energy in the combustor is higher than the total energy abstracted from the fuel. This phenomenon is due to the fact that part of the heat in the exhaust flow is recovered and delivered into the combustion chamber. Within the chamber, the total wall heat transfer of the split cycle engine is lower due to the lower average combustion temperature. This results in a 4% total thermal efficiency improvement in the split cycle engine case. Consequently, the network output in the split cycle engine is significantly increased.

4.4 System efficiency analysis

The theoretical analysis indicates the split cycle engine efficiency is improved by three parameters; the isothermal index C, the regenerator effectiveness σ, and the combustion release heat Q_{LH}. On a real split cycle engine, the cycle efficiency is also affected by losses in the quasi-isothermal compression, the recuperation and the combustion process. These processes were discussed in the previous section based on a one-dimensional engine model. Since the compression process is independent of the recuperation and combustion process, it can be discussed separately. After the separator, the pure air is pre-heated by the recuperator and delivered into the combustion chamber. The property and mass flow rate of the working fluid can then be considered as constant, and the recuperation and combustion process can be analysed together. The overall cycle efficiency improvement on the split cycle engine is the combination of three factors and can be expressed as:

$$E_{impro} = E_{comp} + \underbrace{E_{recup} + E_{comb}}_{Recuperated-combustion} \quad (9)$$

Where E_{impro} is the efficiency improvement of the split cycle engine compared to the conventional diesel engine, expressed as the increase in work for a given fuel input normalised by the fuel input. E_{comp} is the incremental efficiency improvement through the reduction of compression work through the quasi-isothermal process, E_{recup} is the efficiency improvement through the recovery of waste heat through the recuperation process, and the E_{comb} represents the efficiency improvement due to the nearly isobaric combustion. Keeping the compression ratio and air-fuel ratio the same, and maintaining the engine speed at 1200 rpm, the engine energy balance of a split cycle engine and conventional diesel engine are shown in Fig. 11 (a) and (b) respectively. In the split cycle engine, a

5% indicated thermal efficiency improvement can be directly achieved by the quasi-isothermal compression; comparing to diesel engine, a 1% thermal loss can be avoided because of the lower compression temperature. Also, 8% energy can be re-utilized through the recuperation process. Due to the energy re-utilization and heat losses reduction, 53% of the energy from the fuel can be converted to work in the combustion cylinder. Compared to the conventional engine with a break thermal efficiency of 40%, a 32% efficiency improvement (increase in work) can be expected by the split cycle engine. At this stage, a comprehensive optimisation and calibration of the recuperation and combustion parameters has not been done. Comparing the 60% efficiency predicted by pure theoretical analysis reported by Coney [15], the result from this one dimensional model are lower. Further performance improvements can be expected through further system optimization.

5. Conclusions

Based on the theoretical analysis and a one-dimensional engine model, the fundamentals and the performance of the split thermodynamic cycle is evaluated. The major findings of the study are as follows:

1) Isothermal compression in a split cycle engine design, significantly improves the recuperation efficiency of a reciprocating engine, and expands the compression ratio range available for recuperation.

2) A quasi-isothermal compression process can be achieved by injecting a certain amount of water in the compression cylinder and increasing the geometric compression ratio.

3) Recuperation efficiency is improved at higher compression ratios.

4) Isobaric combustion enables a low peak combustion temperature. Given a fixed thermal load constraint, such a low temperature leads to a cycle efficiency improvement and a reduction of wall heat transfer losses.

5) Concerning the whole cycle efficiency, a 53% break thermal efficiency can be expected for split cycle engines, compared to a baseline efficiency of 40% efficiency for a conventional diesel engine.

Acknowledgement

The authors would like to thank the UK's Technology Strategy Board for their co-funding of the Cryopower Project under the IDP8 programme.

References

1. U.S. Census Bureau., *Current industrial reports. MA333L, Internal combustion engines*, 2000, U.S. Census Bureau,: Washington, D.C.
2. Heywood, J.B., *Internal combustion engine fundamentals*. McGraw-Hill series in mechanical engineering. 1988, New York: McGraw-Hill. xxix, 930 p., 2 p. of plates.
3. Caresana, F., et al., *Energy and economic analysis of an ICE-based variable speed-operated micro-cogenerator.* Applied Energy, 2011. **88**(3): p. 659-671.
4. Venkanna, B.K. and C.V. Reddy, *Effect of injector opening pressure on performance, emission and combustion characteristics of DI diesel engine fueled with diesel and honne oil methyl ester.* Environmental Progress & Sustainable Energy, 2013. **32**(1): p. 148-155.
5. Millo, F., et al., *Real CO2 emissions benefits and end user's operating costs of a plug-in Hybrid Electric Vehicle.* Applied Energy, 2014. **114**: p. 563-571.
6. Kang, I., J. Bae, and G. Bae, *Performance comparison of autothermal reforming for liquid hydrocarbons, gasoline and diesel for fuel cell applications.* Journal of Power Sources, 2006. **163**(1): p. 538-546.
7. Farrauto, R.J., *From the internal combustion engine to the fuel cell: Moving towards the hydrogen economy.* Science and Technology in Catalysis 2002, 2003. **145**: p. 21-29.
8. Bishop, J.D.K., N.P.D. Martin, and A.M. Boies, *Cost-effectiveness of alternative powertrains for reduced energy use and CO2 emissions in passenger vehicles.* Applied Energy, 2014. **124**: p. 44-61.
9. Ziviani, D., A. Beyene, and M. Venturini, *Advances and challenges in ORC systems modeling for low grade thermal energy recovery.* Applied Energy, 2014. **121**: p. 79-95.
10. Stanton, D.W., *Systematic Development of Highly Efficient and Clean Engines to Meet Future Commercial Vehicle Greenhouse Gas Regulations.* SAE Int. J. Engines, 2013. **6**(3): p. 1395-1480.
11. Fu, J.Q., et al., *A comparative study on various turbocharging approaches based on IC engine exhaust gas energy recovery.* Applied Energy, 2014. **113**: p. 248-257.
12. Caton, J.A., *Thermodynamic Advantages of Low Temperature Combustion (LTC) Engines Using Low Heat Rejection (LHR) Concepts*, 2011, SAE International.
13. Sprouse, C. and C. Depcik, *Review of organic Rankine cycles for internal combustion engine exhaust waste heat recovery.* Applied Thermal Engineering, 2013. **51**(1-2): p. 711-722.
14. Arcoumanis, C., *Internal combustion engines*. 1988, London: Academic. x, 397 p.
15. Coney, M.W., C. Linnemann, and H.S. Abdallah, *A thermodynamic analysis of a novel high efficiency reciprocating internal combustion engine - the isoengine.* Energy, 2004. **29**(12-15): p. 2585-2600.
16. Sud, K., S. Cetinkunt, and S.B. Fiveland, *Modeling and Validation of a Split Cycle Clean Combustion Diesel Engine Concept.* Journal of Engineering for Gas Turbines and Power-Transactions of the Asme, 2013. **135**(8).
17. Jackson, N.S. and A.F. Atkins, *Split Cycle Reciprocating Piston Engine*, 2012, Google Patents.

18. Yan, X.L. and L.M. Lidsky, *Dual brayton cycle gas turbine pressurized fluidized bed combustion power plant concept.* Journal of Engineering for Gas Turbines and Power-Transactions of the Asme, 1998. **120**(3): p. 566-572.
19. Khaliq, A. and S.C. Kaushik, *Second-law based thermodynamic analysis of Brayton/Rankine combined power cycle with reheat.* Applied Energy, 2004. **78**(2): p. 179-197.
20. Cong, S., C.P. Garner, and G.P. McTaggart-Cowan, *The effects of exhaust back pressure on conventional and low-temperature diesel combustion.* Proceedings of the Institution of Mechanical Engineers Part D-Journal of Automobile Engineering, 2011. **225**(D2): p. 222-235.
21. Incropera, F.P. and D.P. DeWitt, *Fundamentals of heat and mass transfer*. 5th ed. 2002, New York: J. Wiley. xix, 981 p.
22. Chen, D.G., et al., *A Research on Compressed Natural Gas Engine Fuel Supply System for Rapid Prototyping Based on AMEsim.* Applied Energy Technology, Pts 1 and 2, 2013. **724-725**: p. 1317-1323.
23. Wu, Z.W., et al., *Numerical Simulations of TWC Light off Characteristics Based on AMESim.* Industrial Instrumentation and Control Systems, Pts 1-4, 2013. **241-244**: p. 785-788.
24. Najafi, M. and Z. Benjelloun-Dabaghi, *A New Modelica Model and Scicos Simulation for 0D/1D NonlinearComplex Systems.* Oil & Gas Science and Technology-Revue D Ifp Energies Nouvelles, 2008. **63**(6): p. 723-736.
25. Li, M., et al., *Simulation on Static and Dynamic Characteristics of Servovalve.* History of Mechanical Technology and Mechanical Design 2012, 2012. **163**: p. 281-285.
26. Oliveira, S.G., et al., *The importance of control considerations for heat exchanger network synthesis: A case study.* Brazilian Journal of Chemical Engineering, 2001. **18**(2): p. 195-210.

Figure Captions

Figure

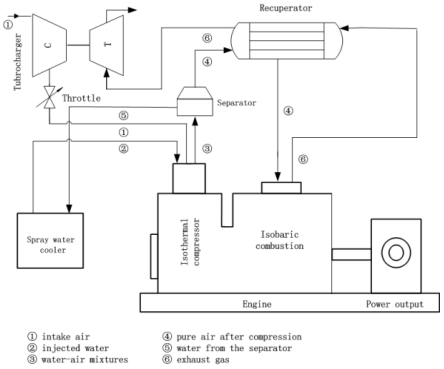

Figure.1 Schematic of the ‘isoengine’ type Split cycle engine

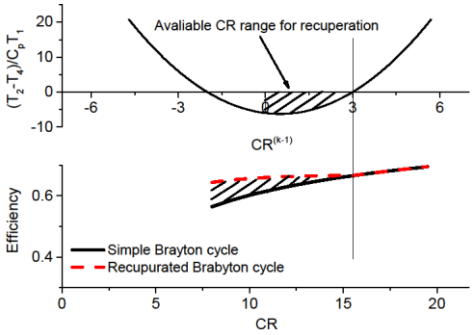

Figure 2. The recuperation available range regarding to the value of CR (Compression ratio)

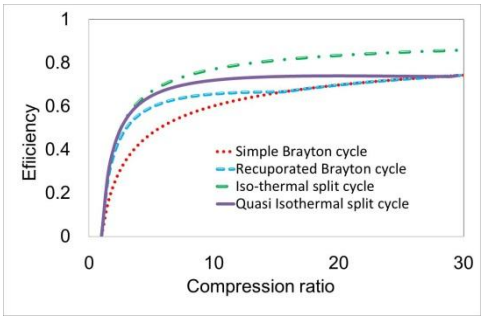

Figure 3. Efficiency comparison of the 4 thermodynamic cycles

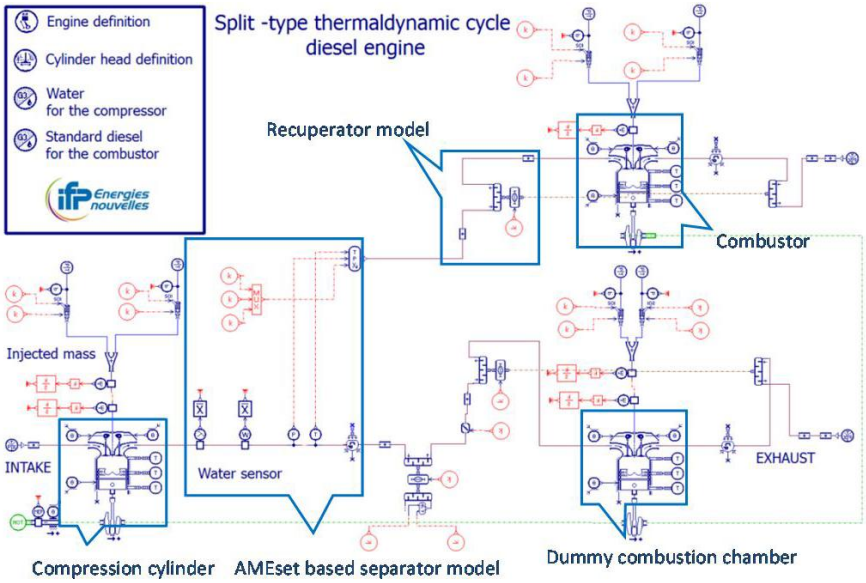

Figure 4. Layout of the Split cycle engine model

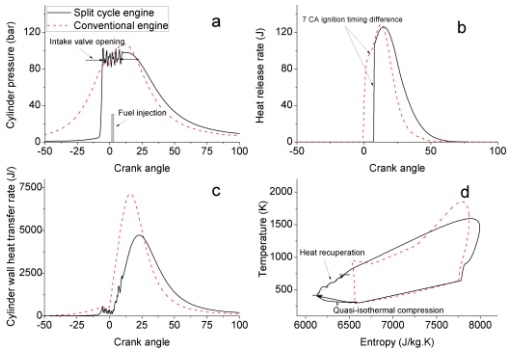

Figure 5. A comparison between the Split cycle engine and the conventional diesel engine

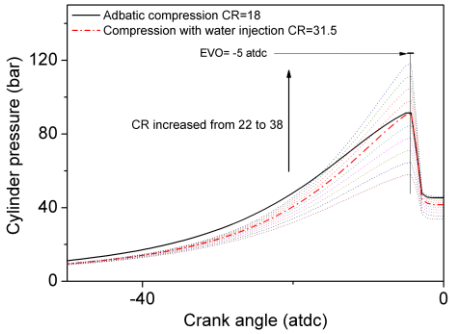

Figure 6. Effect of water injection on the compression process

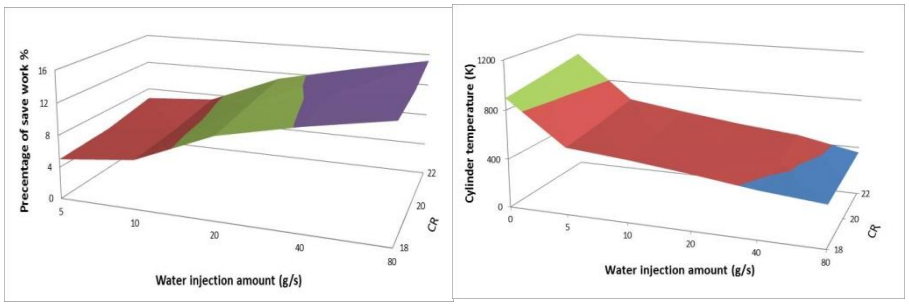

Figure 7. Effect of the water injection rate on (a) the work consumption and (b) in-cylinder temperature

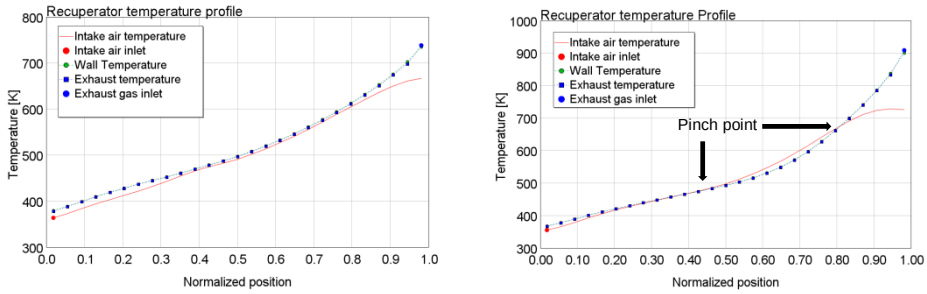

Figure 8. Temperature distributions within the recuperator under the condition of (a) CR=20 and (b) CR=25

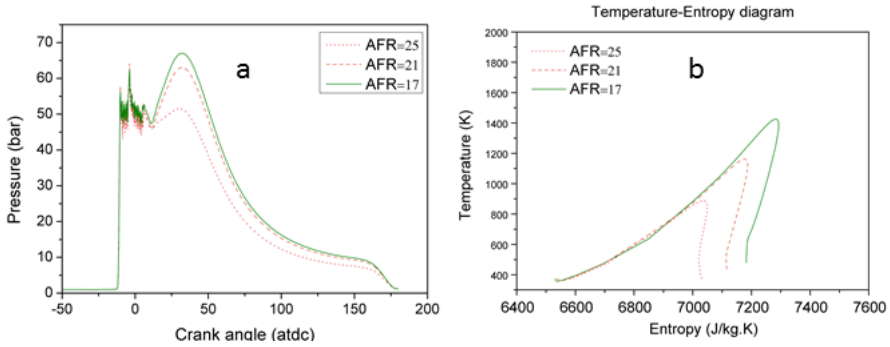

Figure 9. Varying curves of (a) pressure and (b) temperature-entropy with different air-fuel ratios

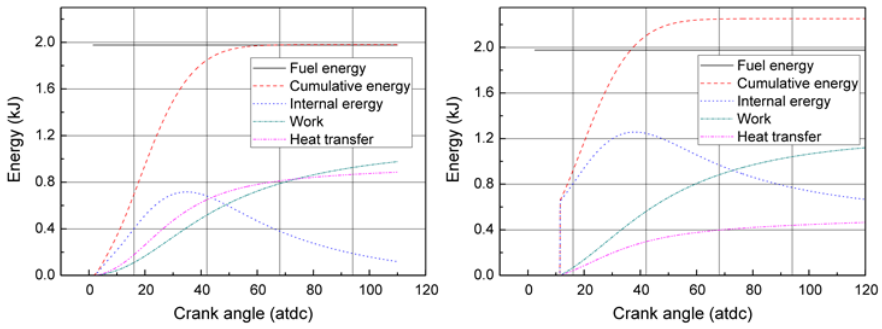

Figure 10. Inner-cylinder energy balances of (a) conventional diesel engine and (b) split cycle engine

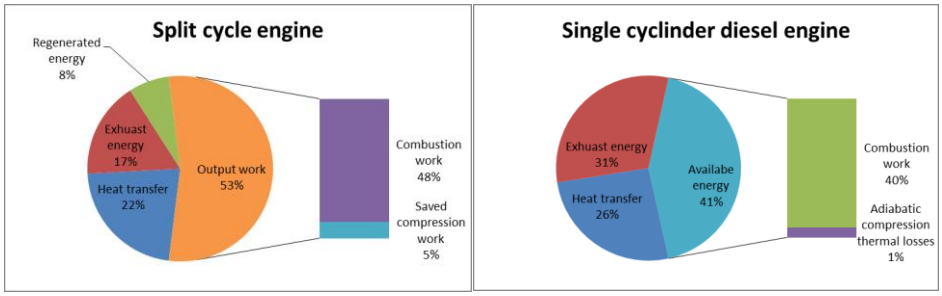

Figure 11. Energy consumption comparison of (a) split cycle engine and (b) conventional diesel engine

Table

Table 1 Comparison of the 4 typical thermo dynamical cycles

	Brayton cycle	Recuperated Brayton cycle	Split cycle with ideal iso-thermal compression	Split cycle with quasi iso-thermal compression
	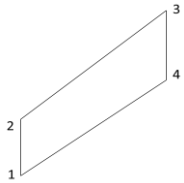	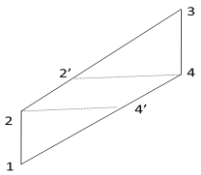	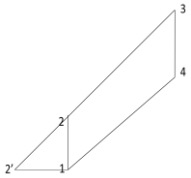	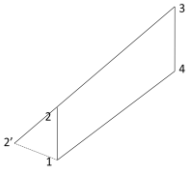
Temperature	$T_1 = T_{amb}$ $T_2 = T_1 \cdot CR^{K-1}$ $T_3 = T_2 + Q_{LH} / Cp$ $T_4 = T_3 / CR^{K-1}$	$T_1 = T_{amb}$ $T_2 = T_1 \cdot CR^{K-1}$ $T_{2'} = T_4$ $T_3 = T_2 + Q_{LH} / C_p$ $T_4 = T_3 / CR^{K-1}$ $T_{4'} = T_2$	$T_1 = T_{amb}$ $T_{2'} = T_1$ $T_2 = T_{2'} + Q_{RE} / C_p$ $T_3 = T_2 + Q_{LH} / C_p$ $T_4 = T_3 / CR^{(K-1)}$	$T_1 = T_{amb}$ $T_{2'} = T_1 \cdot CR^{(K-1)\cdot C}$ $T_2 = T_{2'} + Q_{RE} / C_p$ $T_3 = T_2 + Q_{LH} / C_p$ $T_4 = T_3 / CR^{(K-1)}$ $C = \exp\left[-\frac{ua}{C_p}\left(1-\frac{T_w}{T_1}\right)\Delta t\right] (0 < C < 1)$
Efficiency	$\eta_t = 1 - \frac{1}{CR^{k-1}}$	$\eta_t = 1 - \frac{CR^{k-1}}{CR^{k-1} + Q_{LH} / C_p T_1}$	$\eta_t = B(1-\frac{1}{CR^{k-1}}) - D \cdot \ln(CR^{k-1})$ $B = \frac{\left(1 + (Q_{RE} + Q_{LH}) / (C_p \cdot T_1)\right)}{(Q_{LH}) / (C_p \cdot T_1)}$ $D = \frac{R_g}{C_p(\mathrm{k}-1)}$	$\eta_t = 1 - \left[\frac{CR^{(\mathrm{k}-1)\cdot C-1} - F(1-\frac{1}{CR^{(\mathrm{k}-1)}}) +}{\frac{C_v}{C \cdot C_p}(CR^{(\mathrm{k}-1)\cdot C} - 1)}\right] / \mathrm{E}$ $E = (Q_{LH}) / (C_p \cdot T_1)$ $F = (Q_{RE} + Q_{LH}) / (C_p \cdot T_1)$
Recuperation available range	–	$T_4 > T_2$	$T_4 > T_1$	$T_4 > T_{2'}$

Table 2 Split cycle engine specifications

Stroke Type	2 stroke	IVO	17° BTDC (compression cylinder) 5° BTDC (combustion cylinder)
Number of cylinders	2 (1 compressor + 1 combustor)	IVC	174° BTDC (compression cylinder) 10° ATDC (combustion cylinder)
CR	23	EVO	5° BTDC (compression cylinder) 152° ATDC (combustion cylinder)
Bore [mm]	128	EVC	10° ATDC (compression cylinder) 2° ATDC (combustion cylinder)
Stroke [mm]	148	Speed	1200 rpm

Table 3 Recuperator specifications

Parameter	Units	Value
Total length	mm	600
Inlet connection diameter (master fluid)	mm	40
Outlet connection diameter (master fluid)	mm	40
Number of tubes		35
Inlet tank volume	liter	0.3
Outlet tank volume	liter	0.3
Dry mass of heat exchanger material	kg	0.23
Tube inner diameter	mm	4
Channel inner cross-sectional flow area	mm^2	12.5
Number of channels (in one tube)		1
Shell diameter	mm	35
Inlet connection diameter (slave fluid)	mm	30
Outlet connection diameter (slave fluid)	mm	30
Slave inlet location relative to master		Opposite Side